Phase retrieval in x-ray coherent Fresnel projection-geometry diffraction

Liberato De Caro[a] and Cinzia Giannini
Istituto di Cristallografia-Consiglio Nazionale delle Ricerche (IC-CNR), via Amendola 122/O, I-70126 Bari, Italy

Alessia Cedola, Daniele Pelliccia, and Stefano Lagomarsino
Istituto di Fotonica e Nanotecnologie-Consiglio Nazionale delle Ricerche (IFN-CNR), via Cineto Romano 42, I-00156 Roma, Italy

Werner Jark
Sincrotrone Trieste, S.S. 14 km 163.5, I-34012 Basovizza (TS), Italy

(Received 7 September 2006; accepted 8 December 2006; published online 23 January 2007)

Coherent x-ray diffraction experiments were performed in Fresnel regime, within a line-projection geometry. A planar x-ray waveguide was used to focus coherent cylindrical waves onto a 7.2 μm Kevlar fiber, which acts as a phase object for hard x rays. The phase was retrieved, by using a Fourier-based iterative phasing algorithm, consistent with measured diffraction data and known constraints in real space, with a submicrometer spatial resolution. © *2007 American Institute of Physics*. [DOI: 10.1063/1.2431457]

The ability of tailoring the dimensional regime of individual submicrometer/nanometer objects represents a landmark achievement in materials science. A key aspect of this research field is the development of structural investigation techniques, and relative methodologies for data treatment, to study the structural and morphological aspects of these complex objects. Presently, further possibilities are emerging, related to innovative sources of coherent x rays[1] and to the explosive development of focusing x-ray optics [Fresnel-zone plates,[2] waveguides (WGs),[3] and refractive lenses[4]] which in some favorable cases can transfer the x-ray beam onto the object without degrading the coherence, as it can happen for x-ray WGs. In this framework, coherent x-ray diffraction imaging (CXDI) was intensively studied and applied in the last decade. Phase retrieval techniques, classified as oversampling techniques, were applied to direct Fourier transform the diffraction pattern into the object image.[5]

It has been recently proposed to extend CXDI in near-field Fresnel regime by the introduction of a "distorted object" for the calculation of the coherent diffraction pattern, to take into account the effects of Fresnel fringes.[6,7] A Fresnel-zone construction is embedded on an original object and then Fourier transformed to form a diffraction image. Simulated numerical examples have indicated that, also for near-field coherent diffraction, suitable Fourier-based iterative phasing algorithms may be realized,[6,7] showing interesting advantages both of faster convergence and unambiguous reconstruction with respect to far-field coherent diffraction. A retrieval of the complex field at the focus of an x-ray zone plate[8] and the reconstruction of a nonperiodic gold sample at 24 nm resolution[9] have been also recently obtained just using Fresnel diffraction based algorithms.

In the present letter we show the possibility of quantitatively retrieving, by means of a Fourier-based iterative phasing algorithm, the transmission function of a phase object starting from a coherent x-ray Fresnel diffraction pattern, obtained in projection geometry illuminating the object with a curved wave field. The developed algorithm was tested on a Kevlar fiber illuminated by the coherent cylindrical wave field provided by a planar waveguide.[3,10] We used for this work 12 keV photons, thus extending to the hard x-ray regions and to poor scattering objects the results obtained in Ref. 9 with soft x rays and good gold scatterers. Moreover our experiment is the first example of coherent diffraction using the intrinsically coherent beam produced by an x-ray waveguide, which can work in a wide range of x-ray energies.[11]

We consider the following experimental geometry. The beam emitted by a linelike coherent and monochromatic source of nanosized dimension σ interacts with a sample at a distance d_1 (calculated from the source to the sample center), then it is transmitted towards an area detector oriented perpendicular to the average direction of the transmitted beam, located at a distance d_2 from the center of the sample. The source plane is assumed perpendicular to the mean direction of the emitted beam. The radiation emitted by the source is quasimonochromatic and almost completely coherent. Applying the paraxial approximation of the Fresnel propagators, the field complex amplitude $A(\boldsymbol{u})$ at the detector plane can be calculated using the Fresnel-Kirchoff integral,[10]

$$A(\boldsymbol{u}) = A_0 \exp\left\{\frac{i\pi u^2}{d_2\lambda}\right\} \int d\boldsymbol{r} f_{\text{chirp}}(\boldsymbol{r}) \exp\left\{-\frac{2i\pi \boldsymbol{u}\cdot\boldsymbol{r}}{d_2\lambda}\right\}, \tag{1}$$

where

$$f_{\text{chirp}}(\boldsymbol{r}) = A(\boldsymbol{r}) \exp\left\{\frac{i\pi r^2}{D\lambda}\right\} f(\boldsymbol{r}), \tag{2}$$

$$A(\boldsymbol{r}) = \int d\boldsymbol{s}\Psi(\boldsymbol{s}) \exp\left\{\frac{i\pi s^2}{d_1\lambda}\right\} \exp\left\{\frac{-2i\pi \boldsymbol{r}\cdot\boldsymbol{s}}{d_1\lambda}\right\}, \tag{3}$$

and the defocus distance D is defined as

$$\frac{1}{D} = \frac{1}{d_1} + \frac{1}{d_2}. \tag{4}$$

Here, A_0 is a complex constant; $\Psi(\boldsymbol{s})$ is the complex amplitude emitted by the source and the integral in $d\boldsymbol{s}$ is performed

[a]Electronic mail: liberato.decaro@ic.cnr.it

on its surface S; $\boldsymbol{r}$ is the perpendicular component of the vector that individuates the generic point of the sample, with respect to the direction of the incident (transmitted) beams; and λ is the wavelength. $f(\boldsymbol{r})$ is the complex transmission function of a nearly planar object. Thus, in projection geometry the amplitude observed at the detector plane would be the Fourier transform (FT) of a Fresnel phase-chirped distorted object function,[6,7] modulated in amplitude due to the spatial distribution of the incident complex wave $A(\boldsymbol{r})$ at the object plane [Eq. (3)], related to the complex amplitude emitted by the source $\Psi(\boldsymbol{s})$.

In point- or line-projection geometries[10] one should either experimentally reconstruct the function $\Psi(\boldsymbol{s})$ (Ref. 8) or theoretically evaluate it, if possible. This evaluation may be possible when $d_1 \gg \sigma^2/\lambda$. In this case the incident complex amplitude $A(\boldsymbol{r})$ at the object plane would be given by the FT of the complex amplitude emitted by the source $\Psi(\boldsymbol{s})$. For source sizes on the submicrometer scale (let, say, $\sigma \approx 100$ nm) and hard x rays (let, say, $\lambda \approx 1$ Å), the condition $d_1 \gg \sigma^2/\lambda$ is even fully satisfied at source $\leftrightarrow$ object distances of the order of 1 mm. When the virtual source of the incident beam impinging on the object is an x-ray WG, it is possible to approximate the real $\Psi(\boldsymbol{s})$ with an effective Gaussian source, as shown in Fig. 5 of Ref. 12. For planar (one-dimensional nanosized) WGs this leads to

$$f_{\text{chirp}}(\boldsymbol{r}) = \exp\left\{\frac{i\pi r^2}{D\lambda} - \frac{r^2}{\xi^2}\right\} f(\boldsymbol{r}) \equiv M_{\text{Fr}}(r) f(\boldsymbol{r}), \tag{5}$$

with $\xi^2 \cong d_1^2 \lambda^2 / \sigma^2$ and all real-space constraints applicable to $f(\boldsymbol{r})$ in the object plane may be transferred onto $f_{\text{chirp}}(\boldsymbol{r})$. As usual, the Fourier-space constraints are given by the square root of the measured wave intensity at the detector plane. Thus, one can realize a suitable Fourier-based iterative phasing program for retrieving the unknown function $f(\boldsymbol{r})$, as schematically summarized in the following steps, with u and r the variables of the Fourier and real spaces, respectively, corresponding to the detector and object planes.

(1) Let us start assuming initial values for the unknown phases at the detector plane:[13] $A(u) = |A(u)| e^{i\phi(u)}$.
(2) Fourier-space constraint: $A(u) = |A(u)| e^{i\phi(u)} \rightarrow \sqrt{I(u)}\, e^{i\phi(u)}$.
(3) Inverse Fourier transform: $f_{\text{chirp}}(r) = \text{FT}^{-1}[A(u)]$.
(4) Inverse Fresnel-term correction: $f(r) = M_{\text{Fr}}^{-1}(r) f_{\text{chirp}}(r)$.
(5) Real-space constraint: $f(r) \rightarrow f_{\text{new}}(r)$.
(6) Fresnel-term correction: $f_{\text{new,chirp}}(r) = M_{\text{Fr}}(r) f_{\text{new}}(r)$.
(7) Fourier transform: $A_{\text{new}}(u) = \text{FT}[f_{\text{new,chirp}}(r)]$.
(8) Iterate from step (2) to (7) until a suitable figure of merit (FOM) individuates a possible solution (best trial).

We have considered as test sample a Kevlar fiber with a circular section of radius $R = 7.2$ μm. The measurements were carried out at the beamline BM5 of ESRF. The 12 keV photon beam was monochromatized by a Si(111) monochromator delivering a $\Delta E/E$ of 10^{-4}. The beam size was limited by a slit placed 50 m from the bending magnet source. We used a planar WG in resonant beam coupling mode located 55 m far from the source to condition the beam and to generate a coherent cylindrical beam. The WG had a Be guiding core layer of 130 nm thickness and Mo claddings as described in Ref. 11. The charge-coupled device area detector had a pixel size of 0.625 μm. 4×4 binning was used in the measurements, i.e., the pixel size Δ was 2.5 μm. Figure 1 shows the square root of the diffraction pattern with $d_1 = 0.017$ m and $d_2 = 0.348$ m.

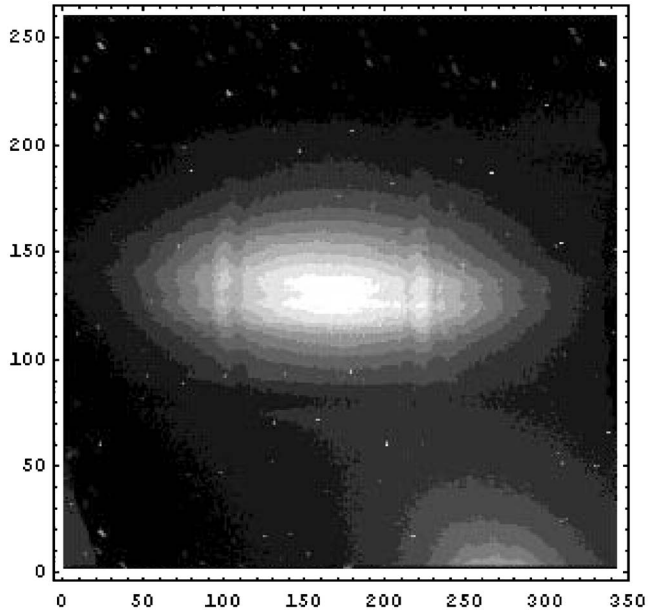

FIG. 1. Square root of the measured diffraction pattern.

At 12 keV ($\lambda = 1.033$ Å), the density of the fiber was 1.44 g/cm^3, the refraction index $n = 1 - 2.1639 \times 10^{-6} + 1.5237 \times 10^{-9} i$, and the fiber can be approximated to a pure phase object. Thus, we can put $f(r) = \exp[i\varphi(r)]$, where $\varphi(r)$ is the phase shift introduced by the fiber, i.e., the unknown function to be retrieved is a complex one. Moreover, in projection geometry the incident beam cannot be stopped and contributes to the overall diffraction pattern. These features imply the need to individuate suitable real- and Fourier-space constraints.

In fact, we consider a one-dimensional phase-retrieval problem (perpendicular to the fiber axis), since we used a planar WG, which generates a Gaussian-like cylindrical wave with its axis parallel to the fiber axis, leading to a line-projection setup.[10] Thus, we averaged the central rows of the measured pattern of Fig. 1 and the obtained result was considered as the one-dimensional Fourier-space constraint regarding the measured wave amplitude perpendicular to the fiber axis.

In the real space we have imposed that the transmission function is equal to 1 out of a region of size $2R$, i.e., $f(r) = 1$ if $r \notin [-R, R]$. In this way we have defined a support suitable for a projection-geometry diffraction experiment on a pure phase object. In fact, in the experimental conditions considered here, it is not possible to impose, as usual, $f(r) = 0$ in a suitable space region surrounding the object. Instead, the *a priori* knowledge in real space is where one should expect $f(r) = 1$. However, the size of this space region ($2R$) cannot *a priori* be fixed for an unknown object, but it can be chosen as a parameter to be determined with the phase-retrieval procedure: in our experiment we should expect that the phasing algorithm would converge when R is sufficiently close to the actual fiber radius.

As initial phases [step (1)] one could assume random phases, but to improve the convergence of the algorithm we have found it useful to start from the Fresnel-term phase values defined in Eq. (5), which constitute a partial *a priori*

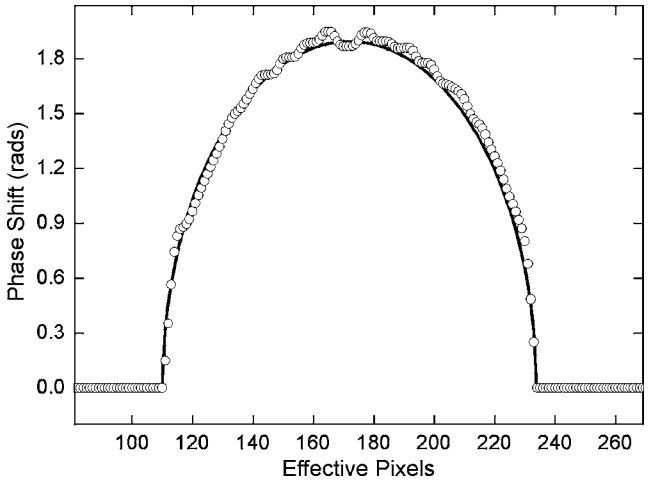

FIG. 2. Circles individuate retrieved values of $\varphi(r)$ in correspondence of the minimum of the FOM; the continuous curve individuates the expected value for an ideal Kevlar fiber with a circular section of 7.2 μm radius.

knowledge about the unknown phase. Thus, we have iterated steps (2)–(7), previously described, and imposed the above constraints for different values of R. The iterations are stopped when the following figure of merit, $\langle \mathrm{FOM} \rangle = |\langle \varphi(r) \rangle - \langle \varphi_R(r) \rangle| / \langle \varphi_R(r) \rangle$, is less than 3%, where the symbol $\langle \cdots \rangle$ indicates the average value, $\varphi_R(r)$ is the phase shift expected for an ideal Kevlar fiber of radius R, and $\varphi(r)$ is the retrieved phase shift. The defined $\langle \mathrm{FOM} \rangle$ is mainly related to the size of the phase object, but it is not influenced by its shape. Thus, the algorithm ends when the size of the support $[-R,R]$ reaches the best match with the measured diffraction data. Moreover, we have also monitored the phasing retrieval by a more detailed figure of merit, sensible to the spatial distribution of the phase shift caused by different beam paths into the object. It is defined as the sum over all the pixels of the deviation of the retrieved phase from the expected values,

$$\mathrm{FOM} = \sum |\varphi(r) - \varphi_R(r)| / \sum \varphi_R(r). \tag{6}$$

The best convergence of the algorithm is obtained for a support of size 14.4 μm ($2R$). This value is in good agreement with the fiber-radius value determined independently both by comparing the measured diffracted intensity transmitted from the fiber with the simulation obtained using the free-space propagation method[14] and by scanning electron microscope measurements. Figure 2 shows the results obtained for the retrieved function $\varphi(r)$ by our phasing algorithm for a support of size of 14.4 μm: the circles individuate retrieved values and the continuous curve individuates the expected value for an ideal Kevlar fiber with a circular section of 7.2 μm radius. In correspondence of this value of R the algorithm executes the minimum number of iterations (only 7) for satisfying the condition $\langle \mathrm{FOM} \rangle < 3\%$. In Fig. 2 the effective pixel size is given by the real pixel size scaled by the magnifying factor $m=(d_1+d_2)/d_1$ due to the projection geometry: $\Delta_{\mathrm{eff}}=\Delta/m$.[10] For our experimental setup the effective pixel size is about 0.12 μm. Let us note, as stressed in Ref. 15, a phase-contrast pattern obtained in projection geometry at a distance $d_2 \gg d_1$ may be compared with a phase contrast obtained by an incident plane wave with the detector in a near-field configuration at a distance d_1. Therefore, as in near-field experiments, the projection geometry allow to bring high spatial frequencies into contrast, even if the detector is far from the sample, while simultaneously maintaining magnification to allow for detector resolution.[15]

In this work we have shown the possibility to quantitatively retrieve with a submicrometer spatial resolution the phase shift of a coherent cylindrical wave exiting by an x-ray WG, after its interaction with a phase object encountered along its path. The coherent diffraction experiments were performed in a Fresnel regime, with hard x rays, within a line-projection geometry, extending to pure phase objects what, very recently,[9] has been done in near field on good x-ray scatters.[9] In our experiment the phase of the object transmission has been retrieved, with a 120 nm spatial resolution, starting from the measured Fresnel diffraction pattern by using a Fourier-based iterative phasing algorithm, imposing known constraints both in real and Fourier spaces, and embedding a Fresnel-zone construction on the complex object transmission function during direct- and inverse-Fourier transform iterative cycles.

The authors thank A. Snigirev and L. Peverini for technical assistance and acknowledge partial financial support from projects SPARC and SPARX.

[1] See, for example, http://xfel.desy.de/
[2] E. Di Fabrizio, F. Romanato, M. Gentili, S. Cabrini, B. Kaulich, J. Susini, and R. Barrett, Nature (London) **401**, 895 (1999).
[3] S. Di Fonzo, W. Jark, S. Lagomarsino, C. Giannini, L. De Caro, A. Cedola, and M. Mueller, Nature (London) **403**, 638 (2000); F. Pfeiffer, C. David, M. Burghammer, C. Riekel, and T. Salditt, Science **297**, 230 (2002); A. Jarre, C. Fuhse, C. Ollinger, J. Seeger, R. Tucoulou, and T. Salditt, Phys. Rev. Lett. **94**, 074801 (2005).
[4] W. Jark, F. Pérennès, M. Matteucci, L. Mancini, F. Montanari, L. Rigon, G. Tromba, A. Somogyi, R. Tucoulou, and S. Bohic, J. Synchrotron Radiat. **11**, 248 (2004); C. G. Schroer and B. Lengeler, Phys. Rev. Lett. **94**, 054802 (2005).
[5] J. Miao, P. Charalambous, J. Kirz, and D. Sayre, Nature (London) **400**, 342 (1999); J. Miao, T. Ishikawa, B. Johnson, E. H. Anderson, B. Lai, and K. O. Hodgson, Phys. Rev. Lett. **89**, 088303 (2002); J. M. Zuo, I. Vartanyants, M. Gao, R. Zhang, and L. A. Nagahara, Science **300**, 1419 (2003).
[6] H. M. Quiney, K. A. Nugent, and A. G. Peele, Opt. Lett. **30**, 1638 (2005).
[7] Xianghui Xiao and Qun Shen, Phys. Rev. B **72**, 033103 (2005).
[8] H. M. Quiney, A. G. Peele, Z. Cai, D. Paterson, and K. A. Nugent, Nat. Phys. **2**, 101 (2006).
[9] G. J. Williams, H. M. Quiney, B. B. Dhal, C. Q. Tran, K. A. Nugent, A. G. Peele, D. Paterson, and M. D. de Jonge, Phys. Rev. Lett. **97**, 025506 (2006).
[10] L. De Caro, C. Giannini, A. Cedola, S. Lagomarsino, and I. Burkreeva, Opt. Commun. **265**, 18 (2006).
[11] W. Jark, A. Cedola, S. Di Fonzo, M. Fiordelisi, S. Lagomarsino, N. V. Kovalenko, and V. A. Chernov, Appl. Phys. Lett. **78**, 1192 (2001).
[12] L. De Caro, C. Giannini, S. Di Fonzo, W. Yark, A. Cedola, and S. Lagomarsino, Opt. Commun. **217**, 31 (2003).
[13] Actually, we need to determine phase shifts of the incident wave after the interaction with object. Therefore, $\phi(u)$ can be determined apart from an arbitrary constant phase.
[14] S. Lagomarsino, A. Cedola, P. Cloetens, S. Di Fonzo, W. Jark, G. Soullie, and C. Riekel, Appl. Phys. Lett. **71**, 2557 (1997).
[15] A. Pogany, D. Gao, and W. S. Wilkins, Rev. Sci. Instrum. **68**, 2774 (1997).